

# High-power distributed Bragg reflector lasers operating at 1065 nm

M. Achtenhagen, N.V. Amarasinghe and G.A. Evans

A report is presented on distributed Bragg reflector lasers emitting in excess of 700 mW in a single-spatial and single-spectral mode at 1065 nm. The threshold current of these devices is  $\sim 30$  mA, there is an L-I slope of 0.74 W/A, and a sidemode suppression ratio greater than 30 dB. The current and thermal tuning are  $0.016 \text{ \AA}/\text{mA}$  and  $0.7 \text{ \AA}/^\circ\text{C}$ , respectively.

**Introduction:** High-power single-frequency laser diodes emitting around 1065 nm are of interest for a variety of applications including direct replacement of Nd:YAG lasers, spectroscopy, gas-sensing or THz generation [1–4]. These first-order distributed Bragg reflector (DBR) ridge waveguide lasers, fabricated with holographic lithography and without regrowth, are expected to have high reliability and low cost in high volume production.

**Fabrication:** The DBR lasers were processed from an MBE grown structure consisting of an n-cladding layer, an InGaAs single quantum well (SQW), which is centred in a 300 nm-thick AlGaAs graded region, a p-cladding layer and a highly-doped GaAs cap layer. A detailed structure and basic processing steps for such ridge-type lasers have been published in [5]. The DBR lasers consist of a 400  $\mu\text{m}$ -long DBR section that provides selective feedback using a first-order grating fabricated by holographic lithography with a grating period of  $\Lambda_B = 1608 \text{ \AA}$ . The grating coupling coefficient is  $50 \text{ cm}^{-1}$  and is controlled by the etch depth. The gain section has a length of 2000  $\mu\text{m}$  and the width of the ridge is  $\sim 3 \mu\text{m}$ . The optical cavity is formed by the rear DBR mirror and a cleaved and coated front facet.

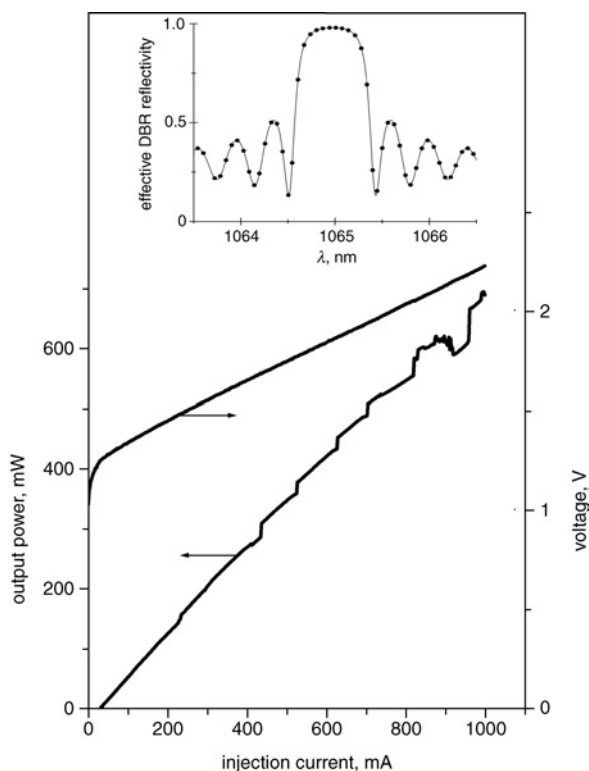


**Fig. 1** Front facet power (*L*) and junction voltage (*V*) against drive current (*I*) of DBR laser operating CW at room temperature

Inset: Effective reflectivity of DBR (solid line) against wavelength; points indicate different stable modes

Following device fabrication, the wafers are thinned to approximately 100  $\mu\text{m}$  and metallised. After bar-cleaving and passivation of the front and rear facet an antireflection coating of around 5% is applied to the front facet. Single devices are separated using conventional dicing techniques and are mounted junction-side down on c-mounts. All

measurements are made under continuous-wave (CW) conditions and at room temperature.

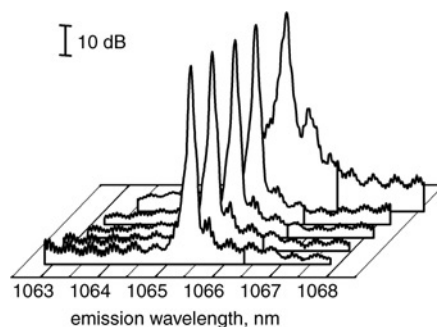


**Fig. 2** Emission spectra from 200 to 600 mW in steps of 100 mW

**Results:** Fig. 1 shows optical power from the front facet and voltage against injection current for a typical DBR device. The device has a threshold current of 30 mA and the slope of the L-I curve above threshold is 0.74 W/A. At a maximum applied injection current of 1.0 A the emitted power exceeds 700 mW. The series resistance  $R_s = 1.0 \Omega$ . Although the devices emit in a single spatial and spectral mode, the L-I curve shows several discontinuities, with the distance between the discontinuities decreasing with increasing current. These discontinuities are associated with small wavelength jumps of  $0.63 \text{ \AA}$ , which correspond to the value for the longitudinal mode spacing (see inset of Fig. 1).

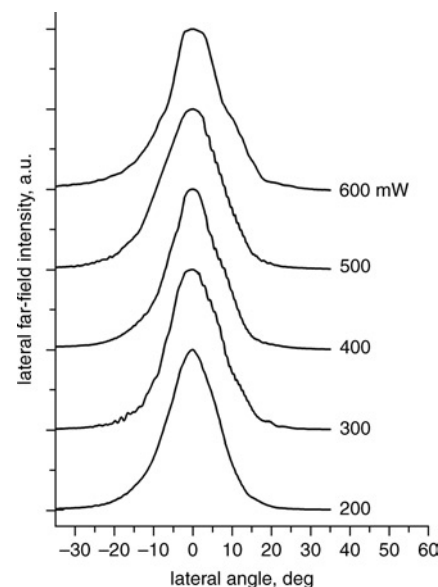


**Fig. 3** Normalised lateral far-field patterns at power levels ranging from 200 to 600 mW in steps of 100 mW

In general, the mode closest to the DBR peak reflectivity has the lowest modal loss and hence becomes the lasing mode. As the injection current and therefore the temperature increases, the modes shift to longer wavelengths, but at a faster rate than the reflectivity spectrum. As the lasing mode moves away from the DBR peak reflectivity, there comes a point where the adjacent mode has a higher reflectivity. At this point the wavelength suddenly jumps to a new mode, resulting in a  $0.63 \text{ \AA}$  decrease in the emission wavelength. Between these mode jumps, the wavelength can be tuned continuously. The inset of Fig. 1 shows the possible different stable modes [6], indicated as solid circles. For this specific example, the DBR has a cleaved end facet (semiconductor–air interface) located at half the grating period. Other DBR cleave locations will be treated below.

The optical spectrum for different power levels is shown in Fig. 2. The full-width at half maximum (FWHM) value of the oscillating mode is limited by the resolution of the optical spectrum analyser ( $0.2 \text{ \AA}$ ). The wavelength tuning rate with current is  $0.016 \text{ \AA}/\text{mA}$  and with temperature is  $0.7 \text{ \AA}/^\circ\text{C}$  measured between 100 and 500 mW. The laser emits in a single spatial and spectral mode with a sidemode suppression ratio exceeding 40 dB for power levels below 550 mW. For

power levels above 550 mW the sidemode suppression ratio decreases to about 30 dB at 600 mW.

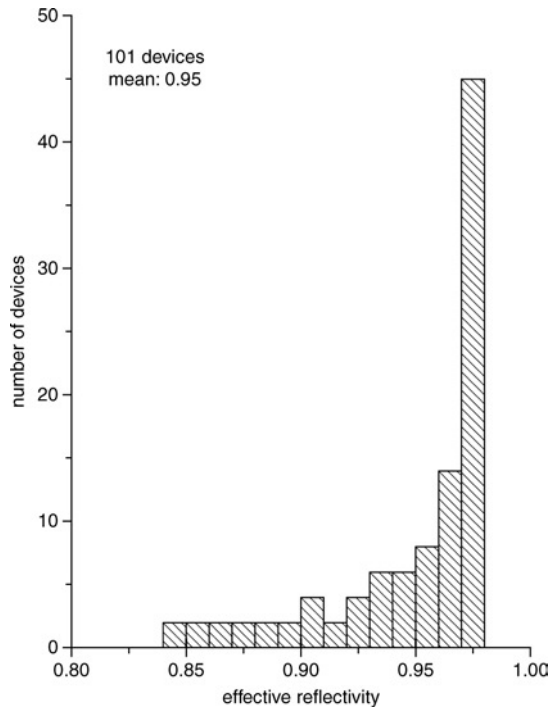


Fig. 4 Calculated distribution of effective DBR reflectivity

Fig. 3 shows the normalised lateral far-field distribution at output powers of 200, 300, 400, 500 and 600 mW. The FWHM of the lateral far-field distribution is about  $12^\circ$  at 200 mW and, due mainly to thermal effects, increases with increasing power. The shape distortion, especially at higher output power is due to the insertion of an attenuator plate in front of the detector. The high power levels required the attenuation of the output beam to prevent detector saturation. The FWHM vertical far-field beam divergence of  $28^\circ$  (not shown) remains almost unchanged over the entire power range.

The residual reflection originating from the semiconductor to air interface at the DBR termination affects the overall reflectivity and depends on the exact location with respect to the grating period. To study this effect we calculated the reflectivity of 101 DBRs including end facet reflectors with varying distance between the facet and the DBR grating period. It is assumed that in practice the cleaving process is random, and produces a similar distribution. Without an end reflector,

the fabricated DBR (power) reflectivity is 93.3%. The inclusion of an end reflector increases the mean value of the effective DBR reflectivity to 95%. Fig. 4 shows the effective reflectivity distribution of the 101 devices. It can be seen that about 45 devices have an effective DBR reflectivity between 96 and 97%.

**Conclusions:** Singlemode, single-frequency DBR lasers have been fabricated with power levels exceeding 700 mW. The emission spectrum of the DBR device tunes quasi-continuously with tuning coefficients of  $0.016 \text{ \AA}/\text{mA}$  and  $0.7 \text{ \AA}/^\circ\text{C}$ . The sidemode suppression ratio is greater than 30 dB over the entire range of operation. Theoretical investigation of the effect of random cleaving positions within the DBR showed that the mean value of the effective DBR reflectivity is increased by 1.7% compared with no end reflector.

**Acknowledgments:** The authors thank S. McWilliams, D. Phan, J. Threadgill, H. Huo and P. Le for processing the laser devices.

© The Institution of Engineering and Technology 2007

23 April 2007

Electronics Letters online no: 20071185

doi: 10.1049/el:20071185

M. Achtenhagen and N.V. Amarasinghe (Photodigm Inc., 1155 E. Collins Blvd., 200, Richardson, TX 75075, USA)

E-mail: machtenhagen@photodigm.com

G.A. Evans (Department of Electrical Engineering, Southern Methodist University, Dallas, TX 75275, USA)

## References

- Hofmann, L., Klehr, A., Bugge, F., Wenzel, H., Smirnitcki, V., Sebastian, J., and Ebert, G.: '180 mW DBR lasers with first-order grating in GaAs emitting at 1062 nm', *Electron. Lett.*, 2000, **36**, (6), pp. 534–535
- Lammert, R.M., Hughes, J.S., Roh, S.D., Osowski, M.L., Jones, A.M., and Coleman, J.J.: 'Low-threshold narrow-linewidth InGaAs-GaAs ridge-waveguide DBR lasers with first-order surface gratings', *IEEE Photonics Technol. Lett.*, 1997, **9**, (2), pp. 149–151
- Hyodo, M., Tani, M., Matsuura, S., Onodera, N., and Sakai, K.: 'Generation of millimetre-wave radiation using a dual-longitudinal-mode microchip laser', *Electron. Lett.*, 1996, **32**, (17), pp. 1589–1590
- Wilk, R., Klehr, A., Mikulics, M., Husek, T., Walter, M., and Koch, M.: 'Terahertz generation with 1064 nm DFB laser diode', *Electron. Lett.*, 2007, **43**, (2), pp. 108–110
- Harder, C., Buchmann, P., and Meier, H.: 'High-power ridge-waveguide AlGaAs GRIN-SCH laser diode', *Electron. Lett.*, 1986, **22**, (20), pp. 1081–1082
- Tromborg, B., Olesen, H., Pan, X., and Saito, S.: 'Transmission line description of optical feedback and injection locking for Fabry-Perot and DFB lasers', *IEEE J. Quantum Electron.*, 1987, **23**, (11), pp. 1875–1889